Nonhomologous End Joining Is Essential for Cellular Resistance to the Novel Antitumor Agent, β-Lapachone

Melissa S. Bentle,[1] Kathryn E. Reinicke,[2] Ying Dong,[3] Erik A. Bey,[3] and David A. Boothman[3]

Departments of [1]Pharmacology and [2]Biochemistry, Case Western Reserve University, Cleveland, Ohio; and [3]Department of Pharmacology, Laboratory of Molecular Stress Responses, and the Simmons Comprehensive Cancer Center, University of Texas Southwestern Medical Center, Dallas, Texas

Abstract

Commonly used antitumor agents, such as DNA topoisomerase I/II poisons, kill cancer cells by creating nonrepairable DNA double-strand breaks (DSBs). To repair DSBs, error-free homologous recombination (HR), and/or error-prone nonhomologous end joining (NHEJ) are activated. These processes involve the phosphatidylinositol 3′-kinase–related kinase family of serine/threonine enzymes: *ataxia telangiectasia* mutated (ATM), ATM- and Rad3-related for HR, and DNA-dependent protein kinase catalytic subunit (DNA-PKcs) for NHEJ. Alterations in these repair processes can cause drug/radiation resistance and increased genomic instability. β-Lapachone (β-lap; also known as ARQ 501), currently in phase II clinical trials for the treatment of pancreatic cancer, causes a novel caspase- and p53-independent cell death in cancer cells overexpressing NAD(P)H:quinone oxidoreductase-1 (NQO1). NQO1 catalyzes a futile oxidoreduction of β-lap leading to reactive oxygen species generation, DNA breaks, γ-H2AX foci formation, and hyperactivation of poly(ADP-ribose) polymerase-1, which is required for cell death. Here, we report that β-lap exposure results in NQO1-dependent activation of the MRE11-Rad50-Nbs-1 complex. In addition, ATM serine 1981, DNA-PKcs threonine 2609, and Chk1 serine 345 phosphorylation were noted; indicative of simultaneous HR and NHEJ activation. However, inhibition of NHEJ, but not HR, by genetic or chemical means potentiated β-lap lethality. These studies give insight into the mechanism by which β-lap radiosensitizes cancer cells and suggest that NHEJ is a potent target for enhancing the therapeutic efficacy of β-lap alone or in combination with other agents in cancer cells that express elevated NQO1 levels. [Cancer Res 2007;67(14):6936–45]

Introduction

Many cancer chemotherapeutic agents, such as ionizing radiation (IR), and DNA-damaging chemotherapeutic compounds cause cell death by creating DNA double-strand breaks (DSBs; refs. 1, 2). DSBs can occur from endogenously produced reactive oxygen species (ROS) or conversion of single-strand breaks (SSBs) to DSBs by advancing replication forks (3). Although cells maintain the capability to survive low levels of DNA damage, as little as one nonrepaired DSB can be lethal (4).

Homologous recombination (HR) and nonhomologous end joining (NHEJ) are two distinct, yet complementary, mechanisms for mammalian DSB repair that can interact simultaneously at DSB sites (5–7). Essential to both HR and NHEJ is the activation of one or all three related phosphatidylinositol 3′-kinase–like kinases (PI3K) in response to DNA damage (7). *Ataxia telangiectasia* mutated (ATM) and ATM- and Rad3-related (ATR) are associated with HR and are typically activated during S-G_2 phase by DNA breaks (e.g., ATM) or after replication fork arrest (e.g., ATR activation). In contrast, DNA-protein kinase catalytic subunit (DNA-PKcs; part of the DNA-PK complex including the Ku70/Ku80 heterodimer) is involved in NHEJ that operates throughout the cell cycle in response to DSBs. These kinases operate as transducer proteins, relaying and amplifying damage signals to mediator proteins. A common substrate of all PI3Ks is the histone variant, H2AX. Formation of phosphorylated H2AX (γ-H2AX) is a sensitive and early marker of DSBs (8, 9). Shortly after DSB detection and PI3K activation, H2AX becomes phosphorylated on serine 139 (γ-H2AX) in a 2-Mb region surrounding the break. Microscopically, this phosphorylation event occurs on a multitude of H2AX molecules leading to foci that are visible when labeled with an antibody specific for γ-H2AX. γ-H2AX foci facilitate the recruitment of DNA damage–regulating protein complexes to the sites of damage (10), whereas γ-H2AX dephosphorylation assists repair (11). The MRE11/Rad50/Nbs-1 (MRN) complex serves as the initial protein complex to participate in both NHEJ and HR repair pathways (12). In NHEJ, the MRN complex modifies DSB ends by its endonuclease and exonuclease activity (13). In HR, the complex acts as an exonuclease to produce 3′ single-strand overhangs bound by Rad52 (12).

β-Lapachone (β-lap; also known as ARQ 501) is currently in phase II clinical trials for the treatment of pancreatic adenocarcinoma in combination with gemcitabine.[4] β-Lap is a novel antitumor agent that is bioactivated by the two-electron oxidoreductase, NAD(P)H quinone oxidoreductase-1 (NQO1; EC 1.6.99.2). Because NQO1 is highly expressed in many human cancers (e.g., pancreatic, breast, lung, and prostate cancers), it is an attractive target for selective cancer chemotherapy by β-lap alone or with IR (14–16). β-Lap–induced cell death is triggered by the NQO1-dependent oxidoreduction of β-lap (14), resulting in a futile cycling wherein β-lap is reduced to an unstable hydroquinone that spontaneously reverts to its parent structure using two oxygen molecules (17). As a result, ROS are generated causing DNA damage, γ-H2AX foci formation, poly(ADP-ribose) polymerase-1 (PARP-1) hyperactivation, and subsequent loss of ATP and NAD^+ (18). β-Lap–induced cell

Note: Supplementary data for this article are available at Cancer Research Online (http://cancerres.aacrjournals.org/).

Requests for reprints: David A. Boothman, Departments of Pharmacology, Oncology and Radiation Oncology, Laboratory of Molecular Stress Responses Program in Cell Stress and Nanomedicine, and the Simmons Comprehensive Cancer Center, University of Texas Southwestern Medical Center, ND2.210K 5323 Harry Hines Boulevard, Dallas, TX 75390. Phone: 214-645-6371; Fax: 214-645-6437; E-mail: David.Boothman@UTSouthwestern.edu.

doi:10.1158/0008-5472.CAN-07-0935

[4] http://clinicaltrials.gov/ct/show/NCT00102700?order=4 and http://clinicaltrials.gov/ct/show/NCT00358930?order=5

death was unique in that PARP-1 and p53 proteolysis occurred concomitant with μ-calpain activation (17). β-Lap–mediated cell death exhibited classic features of apoptosis (e.g., DNA condensation and terminal deoxynucleotidyl transferase-mediated dUTP nick-end labeling–positive cells), but was not dependent on typical apoptotic mediators, such as p53, Bax/Bak, or caspases (19).

To date, few studies explored the contribution of DSB repair in β-lap–induced cell death. We showed that β-lap caused DNA damage, γ-H2AX focus formation and PARP-1 hyperactivation selectively in NQO1-expressing ($NQO1^+$) cells (18). We therefore investigated whether β-lap exposure of $NQO1^+$ cancer cells activated HR and/or NHEJ, and explored the extent to which these repair systems influenced cellular sensitivity. Various model cell systems with altered ATM, ATR, or DNA-PKcs functions, as well as use of selective kinase inhibitors were used. β-Lap caused a delayed (10–15 min) dose-dependent activation of the MRN complex, as well as ATM, DNA-PKcs, and ATR compared with IR. Importantly, only inhibition of DNA-PKcs enhanced β-lap potency, indicating a predominant role for NHEJ in DSB repair, and resistance of cancer cells to this agent. These results suggest the combinatorial use of NHEJ inhibitors to enhance β-lap cytotoxicity for the treatment of human cancers that express elevated NQO1 levels.

Materials and Methods

Reagents. β-Lap was synthesized by Dr. William G. Bornmann (M.D. Anderson Cancer Center, Houston, TX), dissolved in DMSO at 40 mmol/L, and the concentration was verified by spectrophotometry (18). Hoechst 33258, etoposide, and dicoumarol were obtained from Sigma (St. Louis, MO). The DNA-PKcs inhibitor, Nu7026 (2-(morpholin-4-yl)-benzo[*h*]chromen-4-one), and ATM/ATR kinase inhibitor (AAI) were obtained from Calbiochem. They were dissolved in DMSO and used at 10 μmol/L unless otherwise stated. 2-Morpholin-4-yl-6-thianthren-1-yl-pyran-4-one (KU-55933) was synthesized by KuDOS Pharmaceuticals Ltd., dissolved in DMSO, and used at 10 μmol/L.

Cell culture. MCF-7 breast cancer cells were maintained and used as described (14). Human MO59K and MO59J cells, proficient and deficient in both DNA-PK activity and p350 protein, respectively (20), were obtained from Dr. Joan Turner (University of Alberta). U2OS-derived stable cell lines that conditionally regulate wild-type (WT) or kinase-dead ATR (KD-ATR) levels by doxycycline were generously provided by Drs. Paul Nghiem and Stuart L. Schreiber (Harvard University, Cambridge, MA; ref. 21). Recombinant ATM was stably expressed in immortalized human A-T cells using an episomal expression vector (22) and designated: A-T cells ($ATM^{-/-}$) and A-T cells ectopically expressing ATM ($ATM^{+/+}$). MO59K, MO59J, $ATM^{-/-}$, and $ATM^{+/+}$ cells were stably infected using a puromycin-selectable pLPCX retroviral vector alone or one containing the NQO1 cDNA packaged in Phoenix-Ampho cells (23). Uninfected cells were removed by puromycin selection (0.5 μg/mL). However, all experiments were done without selection. NQO1 expression was evaluated in all cells as described (14). All cells were grown in high glucose-containing DMEM containing 10% fetal bovine serum (FBS) or tetracycline-free FBS (U2OS cells), 2 mmol/L L-glutamine, penicillin (100 units/mL), and streptomycin (100 mg/mL) at 37°C in a 5% CO_2, 95% air humidified atmosphere (24). All tissue culture components were purchased from Invitrogen. Cells were free of *Mycoplasma* contamination.

Relative survival assays. Relative survival assays were done as described (14). MCF-7, MO59K, and MO59J cells were pretreated for 1 h with 10 μmol/L Nu7026 or KU-55933 before cotreatment with β-lap at the indicated doses for 2 to 4 h. After β-lap treatment, medium containing Nu7026 or KU-55933 alone was added and then removed after 16 h. Drug-free medium was added and survival was assessed after 6 days. U2OS WT or KD-ATR cells were treated with 1 μg/mL doxycycline 48 h before treatment with various β-lap doses, with or without dicoumarol (40 μmol/L) for 2 to 4 h, then replaced with drug-free medium. Prior studies using β-lap showed that relative survival assays correlated directly with colony-forming ability (14). Data were expressed as means ±SE for treated versus control from separate triplicate experiments, and comparisons were analyzed using a two-tailed Student's *t* test for paired samples.

Cell irradiation. For UV light C (UVC) exposures, U2OS WT and KD-ATR culture medium were removed, and then placed uncovered under a UV lamp emitting primarily 254 nm radiation (fluency rate of 2.2 $J/m^2/s$). After exposure, medium was replaced and cultures incubated for various times. Other cells were treated with 10 μmol/L β-lap or 500 μmol/L H_2O_2 and harvested for immunoblotting 2 h after treatment. For IR, cells were irradiated using a ^{137}Cs source as described and analyzed for foci formation (see below; ref. 25).

Immunoblotting. Western blots were prepared as described (19) with modifications. To examine Chk1, whole-cell extracts were prepared using lysis buffer [50 mmol/L Tris (pH 8.0), 150 mmol/L NaCl, 1 mmol/L EDTA, 1 mmol/L EGTA, 1% NP40, 10 μL/mL protease inhibitor mixture, and 1 mmol/L sodium metavanadate]. Total α-Chk-1 and the α-phospho-Ser345 Chk-1 (Chk1-pSer345) antibody were used at a dilution of 1:100 (Cell Signaling Technology) and α-tubulin was used at a dilution of 1:5,000 (Calbiochem). An NQO1 antibody was generously provided to us by Dr. David Ross (University of Colorado Health Science Center, Denver, CO) and used at a 1:2,000 dilution (26).

Confocal microscopy. MCF-7 cells were treated with 1 to 5 μmol/L β-lap for various times with or without pretreatment and cotreatment with Nu7026, KU-55933, or DMSO. As a positive control for DSB damage responses, cells were irradiated with 5 Gy and fixed 15 min later. After treatment, cells were fixed in methanol/acetone (1:1) and incubated with primary antibodies: α-MRE11, α-Rad50 (GeneTex), α-Nbs-1 phospho-Ser343 (Nbs-1-p; Abcam), α-ATM phospho-Ser1981, α-DNA-PKcs phospho-Thr2609 (Rockland), or α-γ-H2AX (Trevigen; Upstate) overnight at 4°C at 1:100 to 500 dilutions. Alexa Fluor fluorescent secondary antibodies (Molecular Probes) were added for 2 h at room temperature. Nuclei were visualized by Hoechst 33258 staining at 1:3,000 dilution. Confocal images were collected using a ×63 numerical aperture 1.4 oil immersion planapochromat objective at 488 and 594 nm from argon/HeNe1 lasers, respectively, using a Zeiss LSM 510 confocal microscope. All Hoescht 33258-stained nuclear images were collected using a Coherent Mira-F-V5-XW-220 Ti-Sapphire laser tuned at 750 nm. Images shown were representative of experiments done at least thrice. The average number of foci/μ slice was calculated as means ±SE by counting ≥30 cells from three independent experiments. Student's *t* tests were used for comparison.

Alkaline and neutral comet assays. Single-cell gel electrophoretic comet assays were done under alkaline or neutral conditions (18). MCF-7 cells were treated with 5 μmol/L β-lap, 100 μmol/L etoposide, 500 μmol/L H_2O_2, or vehicle alone and harvested at various times. For neutral comet assays, after cellular lysis, slides were immersed in neutral buffer [1 × Tris-borate EDTA (pH 7.0)] for 60 min at room temperature in the dark. Each data point represents the average of 100 cells ±SE, and data are representative of experiments done in duplicate.

Results

MRN complex activation by β-lap. Previously, we showed that exposure of NQO1-expressing cancer cells to β-lap caused ROS and DNA damage, measured by alkaline comet assays and γ-H2AX formation (18). Furthermore, activation of the MRN complex following β-lap exposure was recently reported in *Saccharomyces cerevisiae* (27). We wanted to determine if, and which, DSB repair pathways were activated in response to β-lap by examining MRN complex recruitment. Although the true nature of damage-induced foci has not been elucidated, these protein complexes are suggested to be a visual indication of DNA repair centers (10). Because the MRN complex is central to both

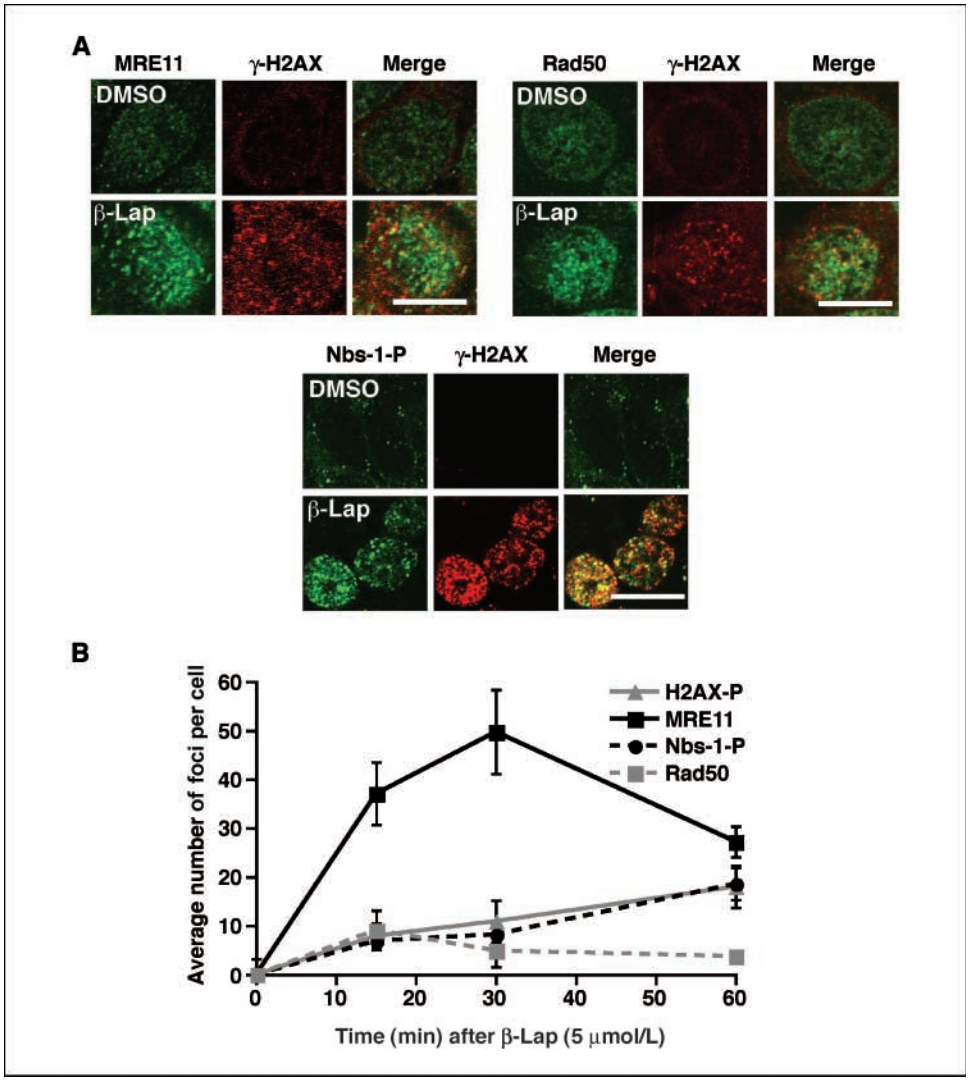

Figure 1. The MRN complex is activated upon β-lap treatment. β-Lap causes punctate nuclear localization of MRE11, Rad50, and phosphorylation of Nbs-1. *A,* visualization of MRE11, Rad50, Nbs-1-p, and γ-H2AX in MCF-7 cells at various times after treatment for 30 min with 5 μmol/L β-lap by confocal microscopy. *B,* average number of MRE11, Rad50, Nbs-1-p, and γ-H2AX foci per cell was determined from ≥60 cells for each treatment group from three independent confocal experiments. *Points,* means; *bars,* SE. Bar, 20 μm.

HR and NHEJ, we examined foci formation in MCF-7 cells after various times of β-lap exposure. Mock- or β-lap–treated cells were stained with antibodies complementary to MRE-11, Rad50, and phosphorylated Ser343 Nbs-1 (Nbs-1-p). Increases in the organized localization of MRE-11 and Rad50 were observed in the nuclei of β-lap–treated cells at 15 min and foci persisted >60 min (Fig. 1*A* and *B*). Similarly, Nbs-1-p nuclear foci were visible beginning 15 min after drug exposure, with similar kinetics as γ-H2AX (Fig. 1*A* and *B*); both proteins are downstream targets of ATM activation (28). MRN complex foci were not visible prior to 15 min β-lap exposure (data not shown). Foci formation was delayed compared with foci observed after IR exposure, in which prior studies have shown γ-H2AX foci formation within 1 to 5 min post-IR (29). Interestingly, with IR-treated cells MRN foci randomly appeared throughout the nucleus, whereas with β-lap–treated cells all components of the MRN formed foci that were predominantly perinuclear (Fig. 1*A*; Supplementary Fig. S1*A*–*C*). The appearance of perinuclear MRN foci is consistent with the fact that NQO1 is largely cytoplasmic (30) and where ROS would diffuse into the nucleus, leading to SSBs. SSBs may then be converted to DSBs at a later time, thereby explaining the delayed activation of the MRN complex.

Dose-dependent activation of ATM and DNA-PK after β-lap treatment. Because the MRN complex was recruited after exposure to β-lap, we examined cells for activation of ATM, a HR-associated PI3K. After interacting with a DSB, ATM undergoes autophosphorylation at serine 1981, causing dissociation of the ATM homodimer (31). Activated ATM monomers phosphorylate numerous downstream proteins, including Nbs-1 (28). To test for ATM activation, MCF-7 cells were mock-treated or exposed to various β-lap doses. Fixed cells were stained with a serine 1981 phosphospecific antibody to ATM (ATM-pSer1981). ATM activation occurred in a dose-dependent manner after β-lap treatment. β-Lap doses (0–3 μmol/L) resulted in few activated ATM molecules, consistent with low levels of DNA damage detected at these doses (Supplementary Fig. S2*A*; Fig. 2*A*). In contrast, lethal doses of β-lap (≥4 μmol/L) caused considerable ATM activation with an ~8-fold increase in the number of foci per cell, corresponding to the net increase in total damage (Supplementary Fig. S2*A*; Fig. 2*A* and *C*). These data suggest that the accumulation of large numbers of β-lap–induced SSBs lead to DSBs that, in turn, activate the canonical HR DSB repair pathway involving MRN and ATM.

Due to the cell cycle independence of NQO1-mediated bioactivation of β-lap (24) and generation of DNA damage, we

examined DNA-PK activation, as it functions in a cell cycle–independent manner (19). Prior work indicated that DNA-PKcs was autophosphorylated at Thr2609 (DNA-PKcs-pThr2609) *in vivo* in response to IR, and DNA-PKcs-pThr2609 colocalizes with γ-H2AX after damage (32, 33). MCF-7 cells were mock-treated or exposed to 1 to 5 μmol/L β-lap for 30 min. Similar to ATM activation, DNA-PKcs-pThr2609 foci formed in a dose-dependent manner. Nontoxic β-lap doses caused few (≥2 foci/cell) DNA-PKcs-pThr2609 foci over background, whereas lethal doses led to increases in DNA-PKcs-pThr2609 foci that colocalized with γ-H2AX (ref. 32; Fig. 2*B*; Supplementary Fig. S2*B*). Importantly, at 3 μmol/L β-lap (~LD_{50} for MCF-7 cells), DNA-PKcs was significantly activated (9 ± 0.2 foci per cell) whereas ATM and γ-H2AX were not as robustly activated (3.9 foci per cell ±1.98 and 3.0 foci per cell ±0.12, respectively). These data suggest that both HR and NHEJ are activated after β-lap exposure, but the predominant DNA repair pathway activated is NHEJ (Fig. 2*C*).

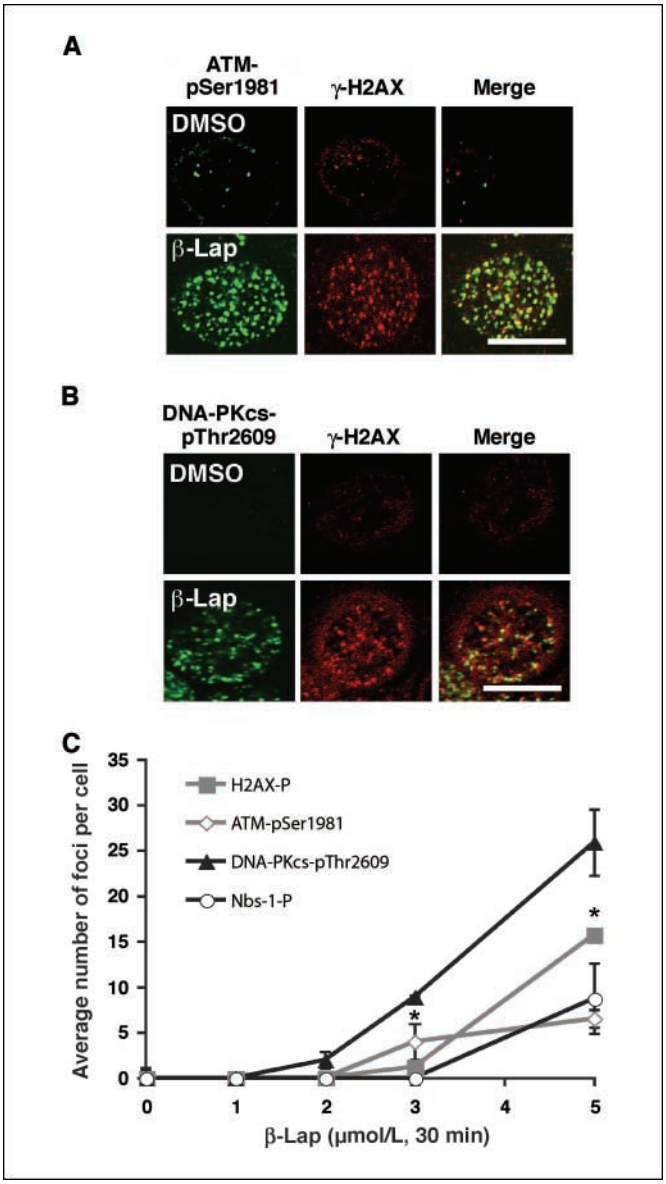

Figure 2. Dose-dependent ATM and DNA-PK activation after β-lap administration. MCF-7 cells were treated with 0 to 5 μmol/L β-lap for 30 min at which time samples were fixed and probed with antibodies to phosphorylated ATM at Ser1981 (*ATM-pSer1981*; *A*) or phosphorylated DNA-PKcs at Thr2609 (*DNA-Pkcs-pThr2609*; *B*) and visualized by confocal microscopy. *C,* MCF-7 cells were treated with 0 to 5 μmol/L β-lap for 30 min; fixed; and probed for ATM-pSer1981, DNA-PKcs-pThr2609, and Nbs-1-p after 30 min. Quantitation of the average number of foci per cell per dose of β-lap–treated cells for ≥60 cells per treatment. *Points,* means; *bars,* SE. Student's *t* test for paired samples, comparing Nbs-1-p or γ-H2AX foci per cell versus the number of DNA-PKcs-pThr2609 foci per cell at various doses of β-lap (*, $P < 0.05$). Bar, 20 μm.

NHEJ is necessary for β-lap–induced cell death. Due to the robust DNA-PK activation after β-lap exposure, we examined the consequences of its inhibition on lethality. Glioblastoma cell lines, MO59K, containing DNA-PKcs and MO59J cells lacking DNA-PKcs, were used (34). These cells lacked NQO1 and were resistant to β-lap. After isolating NQO1-expressing pooled variants, MO59K (MO59K-NQ^+) and MO59J (MO59J-NQ^+) cells had NQO1 enzymatic activities of 790 ± 20 and 690 ± 10 μmol/cytochrome *c* reduced/μg protein, respectively. MO59J-NQ^+ and MO59K-NQ^+ were mock treated or exposed to various β-lap doses for 2 h, with or without dicoumarol cotreatment (a selective NQO1 inhibitor). DNA-PKcs–deficient MO59J-NQ^+ cells were significantly more sensitive to β-lap than their DNA-PKcs–proficient counterparts, MO59K-NQ^+ cells (Fig. 3*A*). MO59J-NQ^+ cells required doses of ~5 μmol/L β-lap to elicit cell death, whereas MO59K-NQ^+ cells were resistant, with only 30% cytotoxicity by 12 μmol/L β-lap. In both cell lines, cytotoxicity was abrogated by inhibiting NQO1 activity with 40 μmol/L dicoumarol (Fig. 3*A*). To assess DNA-PKcs functionality, we pretreated both MO59J-NQ^+ and MO59K-NQ^+ cells with a DNA-PKcs selective inhibitor Nu7026 before β-lap exposure. Nu7026 is a potent radiosensitizer in both proliferating and quiescent cells (35). As anticipated, Nu7026 had little effect on β-lap–induced cell death in MO59J-NQ^+ cells because they are devoid of DNA-PKcs activity. In contrast, Nu7026 significantly sensitized MO59K-NQ^+ cells to β-lap (Fig. 3*B*). Treatment with Nu7026 and 12 μmol/L β-lap resulted in an ~80 ± 3% reduction in survival versus ~5 ± 1% loss of survival in MO59K-NQ^+ cells that were pretreated with vehicle (Fig. 3*B*).

To confirm that DNA-PK was essential in resistance to β-lap–induced cell death, MCF-7 cells were treated with sublethal doses of β-lap with or without pretreatment and cotreatment with 30 μmol/L Nu7026 for 2 h and relative survival was determined. β-Lap doses ≤2 μmol/L had little to no cytotoxicity alone, whereas β-lap doses 2.5 μmol/L and higher caused significant lethality. When MCF-7 cells were treated with Nu7026 and β-lap, lethality was potentiated (Fig. 3*C*). Significant differences in cell death were noted at 2 to 2.5 μmol/L β-lap, where cotreatment with otherwise nontoxic doses of Nu7026 and β-lap resulted in a >80% reduction in survival compared with cells treated with β-lap alone (Fig. 3*C*). To confirm that DNA-PKcs and not ATM was important in β-lap–induced cell death, MCF-7 cells were treated with 5 μmol/L β-lap alone with or without pretreatment and cotreatment with 30 μmol/L Nu7026. Effects on DNA-PKcs versus ATM foci formation were then assessed. After 30 min of β-lap exposure, cells were fixed and stained with antibodies to both DNA-PKcs-pThr2609 and ATM-pSer1981 and the average number of foci per cell were examined by confocal microscopy. β-Lap–treated MCF-7 cells resulted in 14 ± 0.1 DNA-PKcs-pThr2609 foci per cell, which was reduced to 3 ± 1 foci per cell after Nu7026 coadministration (Fig. 3*D*). ATM-pSer1981 foci were not altered after Nu7026 and β-lap treatment versus β-lap alone (5 ± 3 versus 5 ± 0.7, respectively), indicating that DNA-PKcs was the predominate PI3K inhibited after treatment with Nu7026 (Fig. 3*D*).

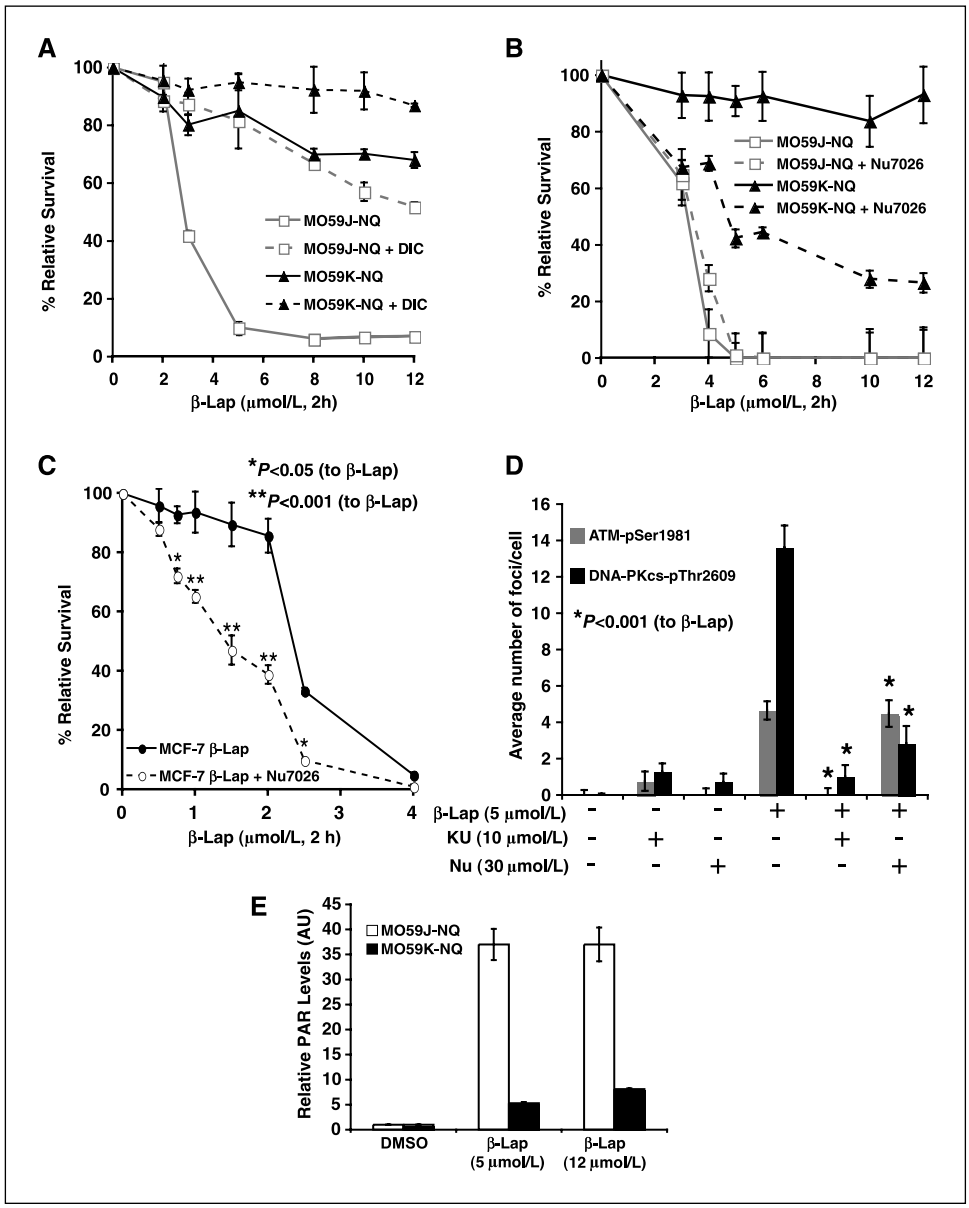

Figure 3. Loss of DNA-PKcs activity potentiates β-lap–induced cell death. *A* to *C,* cell death was examined using relative survival assays in NQO1-containing cells. *A,* MO59K-NQ$^+$ (DNA-PKcs positive) and MO59J-NQ$^+$ (DNA-PKcs negative) cells were treated with varying doses of β-lap alone or in combination with 40 μmol/L dicoumarol (*DIC*) for 2 h. After drug exposure, media were removed and drug-free medium was added. Cells were then allowed to grow for an additional 6 d and relative survival, based on DNA content, was determined by Hoechst 33258 staining as described in Materials and Methods. *B,* loss of DNA-PKcs kinase activity sensitizes MO59K-NQ$^+$ cells to β-lap. Relative survival assays using MO59K-NQ$^+$ and MO59J-NQ$^+$ pretreated and cotreated with the DNA-PKcs inhibitor Nu7026 (10 μmol/L) for 1 h before treatment with varying doses of β-lap for 2 h. *C,* inhibition of DNA-PKcs with Nu7026 potentiates β-lap–induced cell death in NQO1$^+$ MCF-7 cells. MCF-7 cells were treated with sublethal to lethal doses of β-lap alone with or without pretreatment and cotreatment with 30 μmol/L Nu7026 for 2 h. Differences were compared using two-tailed Student's *t* test. Groups having *$P \leq 0.05$ and **$P \leq 0.001$ values compared with β-lap alone are indicated. *D,* Nu7026 inhibits DNA-PKcs-pThr2609 but not ATM-pSer1981. MCF-7 cells were treated with 5 μmol/L β-lap with or without pretreatment and cotreatment with 30 μmol/L Nu7026 for 30 min. After treatment, cells were fixed and probed with antibodies to DNA-PKcs-pThr2609 and ATM-pSer1981 and foci were visualized by confocal microscopy. Quantitation of the average number of foci per cell for at least 60 cells per treatment group. *Columns,* mean; *bars,* SE. Student's *t* test for paired samples, experimental groups containing β-lap + KU55933 (*KU*) or Nu7026 (*NU*) versus β-lap alone. *, $P < 0.001$. *E,* lack of DNA-PKcs causes PARP-1 hyperactivation after β-lap treatment. Immunoblot analyses of PAR and α-tubulin protein levels from whole-cell extracts from MO59J-NQ$^+$ and MO59K-NQ$^+$ cells that were mock treated or treated with 5 or 12 μmol/L β-lap and harvested after 30 min. Relative PAR levels were determined by densitometry analyses using α-tubulin loading controls by NIH ImageJ wherein controls were set to 1.0. *Columns,* means; *bars,* SE. *AU,* arbitrary units.

We previously showed that β-lap–induced cell death was mediated by PARP-1 hyperactivation (18). Because a deficiency in DNA-PKcs potentiated β-lap–induced cell death, we examined whether NHEJ inhibition was accompanied by PARP-1 hyperactivation at sublethal doses of β-lap. PARP-1 is associated with both SSB and DSB repair. After binding to DNA breaks, PARP-1 converts β-NAD$^+$ into polymers of branched or linear poly(ADP-ribose) (PAR) units and attaches them to various nuclear proteins, including PARP-1 itself as part of its autoregulation (36). MO59J-NQ$^+$ and MO59K-NQ$^+$ cells were treated with various doses of β-lap and cell extracts prepared at 20 min posttreatment. Lethal doses of β-lap in MO59J-NQ$^+$ cells resulted in

considerable PAR accumulation, whereas the same dose that was nontoxic to MO59K-NQ$^+$ cells resulted in little PAR accumulation (Fig. 3*E*). Increasing levels of PAR polymers were noted in the MO59K-NQ$^+$ cells with increasing (≥5 μmol/L) β-lap doses (Fig. 3*E*). Treatment of β-lap-exposed MCF-7 cells with Nu7026, but not with the ATM and ATR inhibitors (KU55933 and AAI), resulted in PAR formation (data not shown).

HR-associated PI3K ATM is not necessary for β-lap–induced cell death. Because ATM autophosphorylation was observed after β-lap treatment in NQO1-proficient cancer cells, we investigated whether loss of ATM would alter β-lap–mediated lethality. Isogenic NQO1$^+$ human immortalized fibroblasts from A-T patients deficient in ATM (ATM$^{-/-}$) or proficient via ectopic ATM expression (ATM$^{+/+}$) were used (22). ATM$^{+/+}$ and ATM$^{-/-}$ cells were mock treated or exposed to various β-lap doses with or without dicoumarol for 4 h. There was no observable difference in β-lap–induced lethality between NQO1-proficient ATM$^{+/+}$ or ATM$^{-/-}$ cells, and both cells were protected from lethality by dicoumarol (Fig. 4*A*).

To corroborate these findings, MCF-7 cells were mock treated or exposed to various doses of β-lap in the presence or absence of the ATM kinase inhibitor, KU55933, or the general ATM/ATR inhibitor, AAI, for 2 or 4 h (37). KU55933 inhibited ATM-pSer1981 after β-lap or IR treatments, but did not inhibit NQO1 (Fig. 3*D*; data not shown). Although weak ATM activation was observed after sublethal doses of β-lap, inhibition of ATM by KU55933 or AAI had little effect on β-lap–induced lethality of Figs. 2*A* and 4*B–C*.

ATR activation after β-lap exposure. HR can also be mediated by ATR, which is recruited to ssDNA regions, arising due to replication fork arrest or during the processing of bulky lesions, such as UV photoproducts (38). We reasoned that β-lap could generate ROS-induced SSBs, causing replication fork stalling. Thus, we examined whether ATR activation occurred in response to β-lap by using a set of stable cell lines derived from U2OS cells (human osteosarcoma). These cells are wild-type for p53, have an intact G_1 DNA-damage checkpoint, and allow the doxycycline-inducible expression of either wild-type ATR or a dominant-negative (kinase-dead) ATR point mutant (21). ATR activation was confirmed by monitoring Chk1-pSer345 levels in WT U2OS cells after exposure to UVC or β-lap (Fig. 5*A*). Chk1-pSer345 was muted in U2OS KD-ATR cells after either UVC or β-lap exposures (Fig. 5*A*). Importantly, neither expression of WT ATR or inhibition of ATR by KD-ATR affected the survival of NQO1$^+$ U2OS cells after β-lap exposure (Fig. 5*B*). Administration of dicoumarol abrogated β-lap–induced lethality in both cell lines (Fig. 5*B*).

To confirm our findings that HR was not necessary for β-lap–induced cell death, we treated MCF-7 cells with AAI, an inhibitor of both ATM and ATR, before β-lap exposure. Inhibition of both enzymes was not sufficient to enhance β-lap–mediated cytotoxicity compared with the 80% enhancement observed after inhibition of DNA-PKcs (Figs. 3*C* and 4*C*). These data indicate that ATR signaling is activated after β-lap exposure, but that it is not a predominant factor required for survival.

β-Lap–induced ATR activation and PARP-1 hyperactivation suggested that this compound caused extensive SSBs, whereas MRN, ATM, and DNA-PK foci formation indicated delayed DSB formation. Neutral and alkaline comet assays were done to

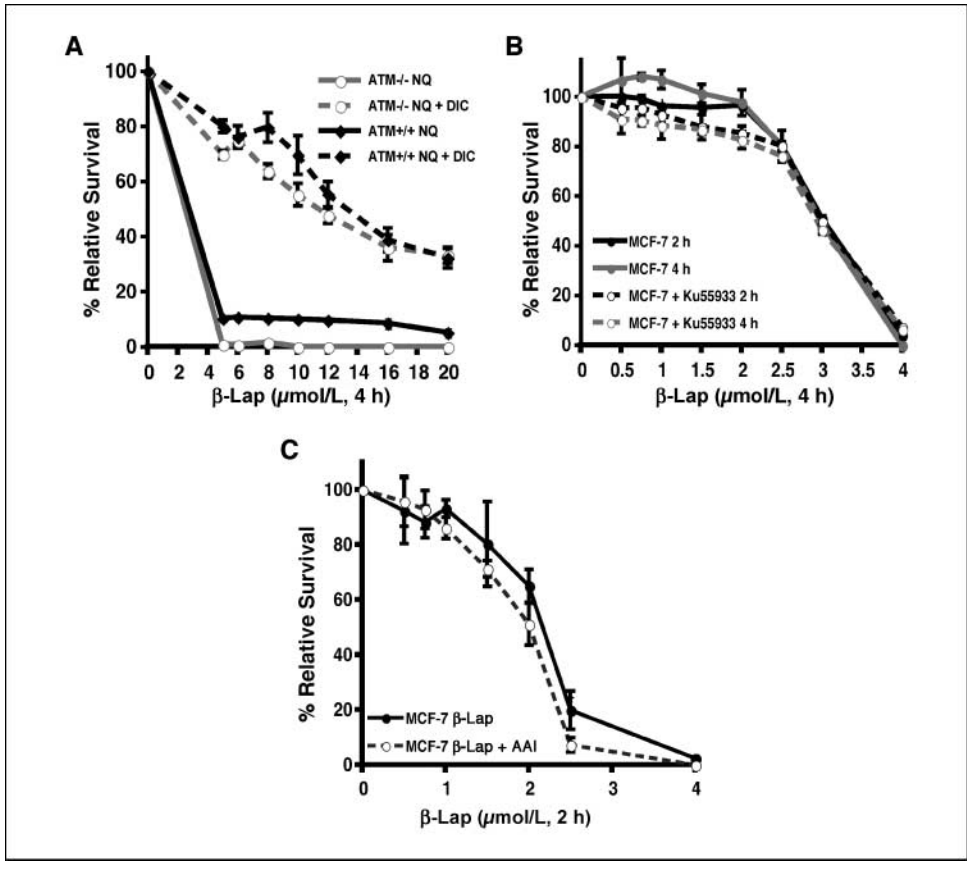

Figure 4. β-Lap–induced cell death is not dependent on ATM. *A* to *C*, cell death was monitored using relative survival assays in NQO1$^+$ cells. *A*, loss of ATM does not potentiate β-lap–induced cell death. NQO1-proficient ATM$^{-/-}$ and ATM$^{+/+}$ cells were treated with varying doses of β-lap alone or in combination with 40 μmol/L dicoumarol for 4 h. MCF-7 cells were treated with 0 to 4 μmol/L β-lap alone or with pretreatment and cotreatment with the ATM kinase inhibitor KU55933 (10 μmol/L) for 2 or 4 h (*B*) or the ATM and ATR kinase inhibitor AAI (10 μmol/L) for 2 h (*C*).

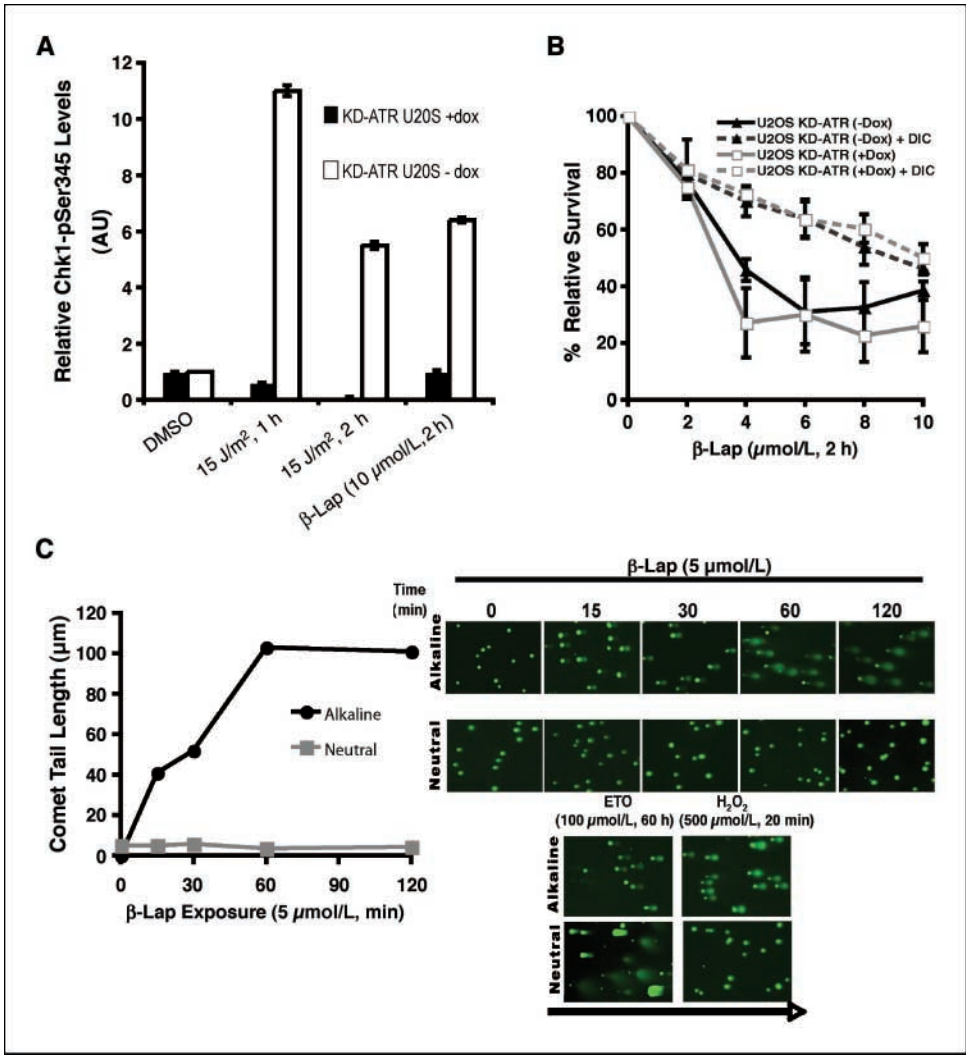

Figure 5. β-Lap causes ATR activation and SSBs. *A,* Chk1-pSer345 occurs after β-lap treatment. Immunoblots of Chk1-pSer345 and α-tubulin protein levels from whole-cell extracts of U2OS KD-ATR treated with or without 1 μg/mL doxycycline for 48 h before treatment with 10 μmol/L β-lap or 15 J/m^2 UVC. Cells were harvested at the indicated times after treatment. Relative Chk1-pSer345 levels were calculated by densitometric analyses by NIH ImageJ using α-tubulin, wherein controls were set to 1.0. *Columns,* means; *bars,* SE. *B,* KD-ATR does not alter cell death caused by β-lap. U2OS KD-ATR cells were treated with or without 1 μg/mL doxycycline (*Dox*) for 48 h to induce expression of the doxycylin-inducible kinase-dead ATR before treatment with varying doses of β-lap alone or in combination with 40 μmol/L dicoumarol for 2 h. *C,* β-lap causes formation of DNA SSBs as shown by comet assays under alkaline and neutral conditions. MCF-7 cells were treated with 5 μmol/L β-lap for 0 to 120 min. At the indicated times during drug treatment, cells were harvested for comet tail formation under either alkaline or neutral conditions. Quantified comet tail lengths of 100 cells for each time and condition calculated using NIH ImageJ software. *Points,* mean; *bars,* SE. *Arrow,* direction of electrophoresis. Not shown: 100 μmol/L etoposide (*ETO*) for 60 h under neutral and alkaline conditions had a comet tail length of roughly 81 ± 4 versus 64 ± 1 μm, respectively.

elucidate the type(s) of breaks created in NQO1-proficient human cancer cells after β-lap exposure. Sublethal doses of β-lap resulted in no detectable DNA strand breakage over time, consistent with their survival (Supplementary Fig. S3; ref. 18). In contrast, lethal doses of β-lap resulted in significant total DNA breaks, occurring immediately after drug exposure at levels surpassing breaks created after 500 μmol/L H_2O_2 (Fig. 5*C*). Prior data showed that ROS formation and DNA damage were detected within ≤5 min after β-lap addition (18). The amount of DNA strand breaks increased over time after 5 μmol/L β-lap treatment, suggesting that the lethal event may be related to the total amount of DNA breaks generated.[5] Interestingly, when cells were analyzed using neutral conditions, little to no DSBs were detected, in contrast to etoposide (ETO) treatment (Fig. 5*C*). As expected, H_2O_2 treatment caused few DSBs, similar to damage observed after β-lap exposure (Fig. 5*C*). The formation of DNA breaks after β-lap treatment was NQO1-dependent because dicoumarol prevented damage (18). These studies indicate that the majority of DNA damage caused by the NQO1-mediated metabolism of β-lap was SSBs, consistent with the genesis of "long-lived" ROS (e.g., H_2O_2).

Discussion

β-Lap, a natural product-based antitumor agent, elicits a unique cell death pathway selectively in cancer cells that express elevated NQO1 levels. The drug is currently in phase I/II clinical trials for the treatment of pancreatic as well as other cancers.[4] We recently showed that β-lap–induced cell death was dependent on PARP-1 hyperactivation, but not on typical apoptotic mediators, such as p53, Bax/Bak or caspases (17). Data from others suggested that β-lap does not cause DNA damage (39). However, we recently showed that β-lap–induced cell death was initiated by the NQO1-dependent generation of ROS, subsequent formation of DNA damage, and calcium-dependent PARP-1 hyperactivation. Once stimulated, PARP-1 hyperactivation depletes ATP/NAD^+ pools inhibiting DNA repair. Therefore, once a threshold level of DNA breaks are formed, PARP-1 hyperactivation appears to be the dominant factor, dictating downstream events leading to cell death (Fig. 6*A*; ref. 18). Because reaching the threshold level of DNA breaks required to hyperactivate PARP-1 is critical for the lethality of this drug, understanding the mechanism(s) by which cells resist

[5] K.E. Reinicke, et al. NAD(P)H:quinone oxidoreductase 1–dependent reactive oxygen species are necessary, but not sufficient, for β-lapachone–mediated cell death, submitted.

this threshold (e.g., amplified DNA repair) is important for improving its efficacy.

To determine the repair pathways activated by β-lap, we examined a number of proteins involved in DSB repair, due to their very rapid and specific localization and modification at DSBs (10). We noted delayed, β-lap–induced MRN complex activation and DNA damage with respect to IR (Figs. 1*A* and *B* and 5; Supplementary Fig. S1). Simultaneously, we noted the activation of ATM and DNA-PK as monitored by their autophosphorylation products, which only occurred in NQO1-expressing cells (Figs. 2*A–C*; Supplementary Fig. S4). Although low levels of γ-H2AX and DNA-PKcs-pThr2609 foci were evident in NQO1-deficient cells, this may be due to the metabolism of this quinone by one-electron oxidoreductases, such as NADPH cytochrome P-450 or b5R reductases (40). Overall, however, these data support a role for NQO1 in amplifying the lethal effects of β-lap via its two-electron oxidoreduction (Supplementary Fig. S4). Activation of ATM, DNA-PK, and the MRN complex were dose-dependent (Figs. 1 and 2). Evidence from our laboratory suggested that this may be due to a minimal threshold of DNA damage created after β-lap treatment, after which point the cell is committed to death via PARP-1 hyperactivation.[5]

DNA-PKcs plays a direct role in DSB repair by acting as a key component of NHEJ because defects in kinase activity result in radiosensitivity (34). Because NHEJ is the primary mechanism by which mammalian cells repair DSBs, we tested the hypothesis that NHEJ was not only activated after β-lap treatment, but necessary to protect cells from β-lap–induced lethality at sublethal doses. We noted an ~2-fold increase in the number of DNA-PKcs-pThr2609 versus ATM-pSer1981–induced foci after β-lap exposure (Fig. 2*C*). Further examination of MO59K-NQ$^+$ and MO59J-NQ$^+$ cells revealed that NHEJ was essential for survival of cells after β-lap treatment (Fig. 3*A*). Importantly, cotreatment of cells with β-lap + Nu7026, a DNA-PKcs inhibitor, sensitized MO59K-NQ$^+$ cells as well as MCF-7 cells (Fig. 3*B* and *C*), indicating a major role for NHEJ in repair of β-lap–induced DNA damage.

To determine if NHEJ inhibition enhanced PARP-1–mediated cell death at otherwise sublethal β-lap doses, we examined PAR accumulation in MO59J-NQ$^+$ and MO59K-NQ$^+$ cells. In DNA-PKcs–deficient MO59J-NQ$^+$ cells, doses of β-lap ≥5 μmol/L alone caused significant PAR modification (Fig. 3*E*). However, the proficiency of NHEJ in MO59K-NQ$^+$ cells muted PAR accumulation, consistent with its role as a cellular resistance factor in β-lap–induced lethality (Fig. 3*E*). Coadministration of Nu7026 in MCF-7 cells converted sublethal β-lap doses into a cytotoxic event accompanied by the accumulation of PAR polymers not seen with ATM or ATR inhibitors (Figs. 3*C* and 4*B* and *C*; and data not shown). These data indicate that interruption of NHEJ during β-lap treatment commits cells to PARP-1–mediated cell death (Fig. 6; ref. 18). A relationship between DNA-PK and PARP-1 has been established, and inhibition of both proteins increased net DSB over time after chemically induced damage (41, 42). Thus, combining β-lap and NHEJ inhibitors would be an ideal "two-hit" cancer therapy, by inhibiting mechanistically diverse DNA repair enzymes and thereby retarding DSB rejoining.

In addition to DNA-PKcs-pThr2609, ATM-pSer1981 was also noted after β-lap treatment (Fig. 2*A*). Although there is some discrepancy as to the exact role ATM plays in HR, it does play a pivotal role in general damage signaling, cell cycle regulation, and the slow component of DSB repair (43–45). After IR, A-T cells fail to show recovery from damage, and experiments using reverse genetics failed to see potentiation in cell death arising from the conditional loss of RAD54 in ATM$^{-/-}$ cells, suggesting an inherent HR defect in ATM$^{-/-}$ cells (46). An interplay between ATM and DNA-PKcs may be important for the proper initiation of DSB signaling and processing of DSBs to ensure repair and maintenance of genomic integrity after damage (47). Using cells deficient in ATM, we tested whether the loss of ATM, and therefore, HR-mediated repair, would alter β-lap–mediated cell death similar to that observed with NHEJ loss. Data from our studies revealed no significant difference between ATM$^{+/+}$ and ATM$^{-/-}$ cells in terms of β-lap sensitivity (Fig. 4*A*). Studies using KU55933 corroborated these findings, as inhibition of ATM did not augment lethality in β-lap–treated MCF-7 cells (Fig. 4*B*). The dose of KU55933 used in these studies was sufficient to inhibit ATM-pSer1981 after IR or β-lap–induced DNA damage (Fig. 3*D*). Interestingly, inhibition of ATM-pSer1981 by this inhibitor also abrogated DNA-PKcs-pThr2609, as recently noted by Chen et al. (47), supporting a role for ATM in DNA-PKcs-pThr2609 in response to DNA damage (Fig. 3*D*). In contrast, inhibition of

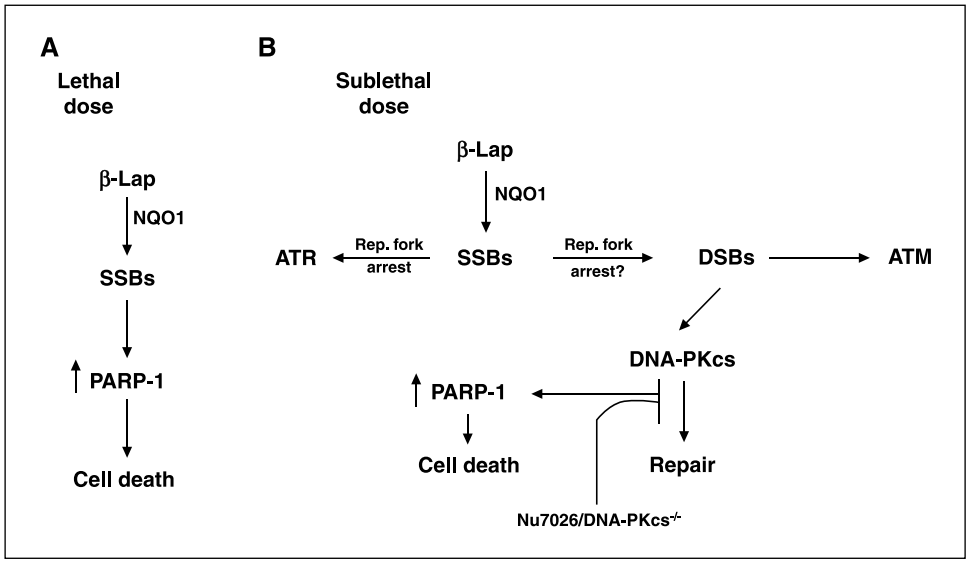

Figure 6. Model of β-lap–induced cell death after lethal and sublethal doses. *A,* β-lap–induced cell death at lethal doses is PARP-1 dominated. β-Lap–mediated metabolism by NQO1 generates ROS that cause SSBs. Extensive SSBs cause hyperactivation of PARP-1 and subsequent NAD$^+$ and ATP loss, which inhibits DNA repair and causes cell death. *B,* nonlethal doses of β-lap are converted to lethal events via DNA-PK inhibition. At sublethal doses of compound, repairable amounts of SSBs are generated, some of which may be converted to DSBs possibly via replication fork arrest. This causes the activation of members of the PI3K family of kinases, ATM, ATR, and DNA-PKcs. However, only NHEJ seems to be the primary repair pathway needed to resolve DSBs after drug treatment, as only inhibition of DNA-PKcs by either chemical (Nu7026) or genetic (DNA-PKcs$^{-/-}$) means potentiated the toxicity of sublethal doses of β-lap leading to PARP-1–mediated cell death.

DNA-PKcs with Nu7026 blocked ATM-mediated DNA-PKcs-pThr2609 (Fig. 3*D*). These data suggested that ATM-mediated DNA-PKcs-pThr2609 was a component of an amplification scheme, whereby autophosphorylation of DNA-PKcs at Thr2609 was required before signal amplification via ATM.

ATR is recruited by ATR-interacting protein to replication protein A–coated ssDNA that accumulates at stalled DNA replication forks or is generated by processing initial DNA damage (28). Thus, ATR activation in response to β-lap exposure may be consistent with stalled replication forks and could indicate the formation of DSBs from SSBs in response to β-lap exposure (48, 49). The primary lesions generated after β-lap exposure were SSBs (Fig. 5*C*). The lack of detectable DSBs could be the result of the low sensitivity of neutral comet assays compared with γ-H2AX–induced foci formation to detect minor DSBs populations. Importantly, formation of γ H2AX, as well as activation of MRN, ATM, DNA PK, and ATR appeared in a delayed manner with respect to initial SSBs (<5 min versus 10–15 min, respectively; ref. 18). These data support the hypothesis that DSBs are formed as a secondary DNA lesion after initial SSBs were generated, likely resulting from stalled replication forks (Fig. 6).

Nevertheless, ATR signaling does not seem to be a factor in β-lap resistance. Using U2OS KD-ATR and WT-ATR, we showed an increase in Chk1-pSer345 after UVC, as well as after β-lap treatment, that was muted in the presence of doxycycline, which increased dominant-negative ATR expression (Fig. 5*A*). Total levels of Chk1 and NQO1 were relatively unchanged under doxycycline treatment (data not shown). U2OS KD-ATR cells treated with or without doxycycline showed no enhanced β-lap toxicity (Fig. 5*B*). Furthermore, addition of AAI had no apparent effect on β-lap–induced cytotoxicity in MCF-7 cells (Fig. 4*C*). Thus, neither ATM nor ATR seem to play major roles as resistance factors in β-lap lethality.

Currently used cancer chemotherapeutic agents function primarily as nonselective inducers of DSBs in highly proliferative cells. A major problem with many of these agents is their lack of selectivity, in which both normal and cancerous tissues are targeted. In contrast, β-lap, which is currently under investigation in phase I/II clinical trials, selectively targets cancer cells that express elevated NQO1 levels, resulting in DNA damage and cell death mediated by PARP-1 (18). Here, we show that in addition to SSB-induced DNA repair pathways, β-lap activates various DSB repair pathways. In particular, NHEJ was a key factor in the survival of cells exposed to β-lap, because inhibition of NHEJ causes PARP-1–mediated cell death after treatment or sublethal doses of β-lap. In summary, these data warrant the combinatorial use of β-lap with inhibitors of NHEJ thereby increasing the therapeutic efficacy of this compound by targeting two distinct repair mechanisms, NHEJ and PARP-1.

Acknowledgments

Received 3/12/2007; accepted 5/8/2007.

Grant support: NIH/National Cancer Institute grant CA10279201 (D.A. Boothman), CWRU Core grant P30CA43703-12, and Department of Defense Breast Cancer Program Predoctoral Fellowships W81XWH-04-1-0301 (M.S. Bentle) and W81XWH-05-1-0248 (K.E. Reinicke).

The costs of publication of this article were defrayed in part by the payment of page charges. This article must therefore be hereby marked *advertisement* in accordance with 18 U.S.C. Section 1734 solely to indicate this fact.

References

1. Krasin F, Hutchinson F. Repair of DNA double-strand breaks in *Escherichia coli*, which requires recA function and the presence of a duplicate genome. J Mol Biol 1977;116:81–98.
2. D'Andrea AD, Haseltine WA. Modification of DNA by aflatoxin B1 creates alkali-labile lesions in DNA at positions of guanine and adenine. Proc Natl Acad Sci U S A 1978;75:4120–4.
3. Kuzminov A. Single-strand interruptions in replicating chromosomes cause double-strand breaks. Proc Natl Acad Sci U S A 2001;98:8241–6.
4. Rich T, Allen RL, Wyllie AH. Defying death after DNA damage. Nature 2000;407:777–83.
5. van Gent DC, Hoeijmakers JH, Kanaar R. Chromosomal stability and the DNA double-stranded break connection. Nat Rev Genet 2001;2:196–206.
6. Richardson C, Jasin M. Coupled homologous and nonhomologous repair of a double-strand break preserves genomic integrity in mammalian cells. Mol Cell Biol 2000;20:9068–75.
7. Khanna KK, Jackson SP. DNA double-strand breaks: signaling, repair and the cancer connection. Nat Genet 2001;27:247–54.
8. Rogakou EP, Pilch DR, Orr AH, Ivanova VS, Bonner WM. DNA double-stranded breaks induce histone H2AX phosphorylation on serine 139. J Biol Chem 1998;273:5858–68.
9. Foster ER, Downs JA. Histone H2A phosphorylation in DNA double-strand break repair. FEBS J 2005;272:3231–40.
10. Paull TT, Rogakou EP, Yamazaki V, Kirchgessner CU, Gellert M, Bonner WM. A critical role for histone H2AX in recruitment of repair factors to nuclear foci after DNA damage. Curr Biol 2000;10:886–95.
11. Chowdhury D, Keogh MC, Ishii H, Peterson CL, Buratowski S, Lieberman J. γ-H2AX dephosphorylation by protein phosphatase 2A facilitates DNA double-strand break repair. Mol Cell 2005;20:801–9.
12. Jackson SP. Sensing and repairing DNA double-strand breaks. Carcinogenesis 2002;23:687–96.
13. Trujillo KM, Yuan SS, Lee EY, Sung P. Nuclease activities in a complex of human recombination and DNA repair factors Rad50, Mre11, and p95. J Biol Chem 1998;273:21447–50.
14. Pink JJ, Planchon SM, Tagliarino C, Varnes ME, Siegel D, Boothman DA. NAD(P)H:quinone oxidoreductase activity is the principal determinant of β-lapachone cytotoxicity. J Biol Chem 2000;275:5416–24.
15. Boothman DA, Pardee AB. Inhibition of radiation-induced neoplastic transformation by β-lapachone. Proc Natl Acad Sci U S A 1989;86:4963–7.
16. Suzuki M, Amano M, Choi J, et al. Synergistic effects of radiation and β-lapachone in DU-145 human prostate cancer cells *in vitro*. Radiat Res 2006;165:525–31.
17. Bentle MS, Bey EA, Dong Y, Reinicke KE, Boothman DA. New tricks for old drugs: the anticarcinogenic potential of DNA repair inhibitors. J Mol Histol 2006;37:203–18.
18. Bentle MS, Reinicke KE, Bey EA, Spitz DR, Boothman DA. Calcium-dependent modulation of poly(ADP-ribose) polymerase-1 alters cellular metabolism and DNA repair. J Biol Chem 2006;281:33684–96.
19. Wuerzberger SM, Pink JJ, Planchon SM, Byers KL, Bornmann WG, Boothman DA. Induction of apoptosis in MCF-7:WS8 breast cancer cells by β-lapachone. Cancer Res 1998;58:1876–85.
20. Lees-Miller SP, Godbout R, Chan DW, et al. Absence of p350 subunit of DNA-activated protein kinase from a radiosensitive human cell line. Science 1995;267:1183–5.
21. Nghiem P, Park PK, Kim Ys YS, Desai BN, Schreiber SL. ATR is not required for p53 activation but synergizes with p53 in the replication checkpoint. J Biol Chem 2002;277:4428–34.
22. Ziv Y, Bar-Shira A, Pecker I, et al. Recombinant ATM protein complements the cellular A-T phenotype. Oncogene 1997;15:159–67.
23. Patton JT, Mayo LD, Singhi AD, Gudkov AV, Stark GR, Jackson MW. Levels of HdmX expression dictate the sensitivity of normal and transformed cells to Nutlin-3. Cancer Res 2006;66:3169–76.
24. Pink JJ, Wuerzberger-Davis S, Tagliarino C, et al. Activation of a cysteine protease in MCF-7 and T47D breast cancer cells during β-lapachone-mediated apoptosis. Exp Cell Res 2000;255:144–55.
25. Boothman DA, Meyers M, Fukunaga N, Lee SW. Isolation of X-ray-inducible transcripts from radioresistant human melanoma cells. Proc Natl Acad Sci U S A 1993;90:7200–4.
26. Siegel D, Franklin WA, Ross D. Immunohistochemical detection of NAD(P)H:quinone oxidoreductase in human lung and lung tumors. Clin Cancer Res 1998;4:2065–70.
27. Menacho-Marquez M, Murguia JR. β-lapachone activates a Mre11p-Tel1p G1/S checkpoint in budding yeast. Cell Cycle 2006;5:2509–16.
28. Kurz EU, Lees-Miller SP. DNA damage-induced activation of ATM and ATM-dependent signaling pathways. DNA Repair (Amst) 2004;3:889–900.
29. Rothkamm K, Lobrich M. Evidence for a lack of DNA double-strand break repair in human cells exposed to very low X-ray doses. Proc Natl Acad Sci U S A 2003;100:5057–62.
30. Winski SL, Koutalos Y, Bentley DL, Ross D. Subcellular localization of NAD(P)H:quinone oxidoreductase 1 in human cancer cells. Cancer Res 2002;62:1420–4.
31. Bakkenist CJ, Kastan MB. DNA damage activates ATM through intermolecular autophosphorylation and dimer dissociation. Nature 2003;421:499–506.
32. Chan DW, Chen BP, Prithivirajsingh S, et al. Autophosphorylation of the DNA-dependent protein kinase catalytic subunit is required for rejoining of DNA double-strand breaks. Genes Dev 2002;16:2333–8.

33. Ding Q, Reddy YV, Wang W, et al. Autophosphorylation of the catalytic subunit of the DNA-dependent protein kinase is required for efficient end processing during DNA double-strand break repair. Mol Cell Biol 2003;23:5836–48.

34. Allalunis-Turner MJ, Barron GM, Day RS III, Dobler KD, Mirzayans R. Isolation of two cell lines from a human malignant glioma specimen differing in sensitivity to radiation and chemotherapeutic drugs. Radiat Res 1993;134:349–54.

35. Veuger SJ, Curtin NJ, Richardson CJ, Smith GC, Durkacz BW. Radiosensitization and DNA repair inhibition by the combined use of novel inhibitors of DNA-dependent protein kinase and poly(ADP-ribose) polymerase-1. Cancer Res 2003;63:6008–15.

36. Kim MY, Zhang T, Kraus WL. Poly(ADP-ribosyl)ation by PARP-1: "PAR-laying" NAD+ into a nuclear signal. Genes Dev 2005;19:1951–67.

37. Hickson I, Zhao Y, Richardson CJ, et al. Identification and characterization of a novel and specific inhibitor of the ataxia-telangiectasia mutated kinase ATM. Cancer Res 2004;64:9152–9.

38. Cortez D, Guntuku S, Qin J, Elledge SJ. ATR and ATRIP: partners in checkpoint signaling. Science 2001;294:1713–6.

39. Pardee AB, Li YZ, Li CJ. Cancer therapy with β-lapachone. Curr Cancer Drug Targets 2002;2:227–42.

40. Byczkowski JZ, Gessner T. Inhibition of the redox cycling of vitamin K3 (menadione) in mouse liver microsomes. Int J Biochem 1988;20:1073–9.

41. Boulton S, Kyle S, Durkacz BW. Interactive effects of inhibitors of poly(ADP-ribose) polymerase and DNA-dependent protein kinase on cellular responses to DNA damage. Carcinogenesis 1999;20:199–203.

42. Ruscetti T, Lehnert BE, Halbrook J, et al. Stimulation of the DNA-dependent protein kinase by poly(ADP-ribose) polymerase. J Biol Chem 1998;273:14461–7.

43. Kuhne M, Riballo E, Rief N, Rothkamm K, Jeggo PA, Lobrich M. A double-strand break repair defect in ATM-deficient cells contributes to radiosensitivity. Cancer Res 2004;64:500–8.

44. Riballo E, Kuhne M, Rief N, et al. A pathway of double-strand break rejoining dependent upon ATM, Artemis, and proteins locating to γ-H2AX foci. Mol Cell 2004;16:715–24.

45. Shiloh Y. The ATM-mediated DNA-damage response: taking shape. Trends Biochem Sci 2006;31:402–10.

46. Morrison C, Sonoda E, Takao N, Shinohara A, Yamamoto K, Takeda S. The controlling role of ATM in homologous recombinational repair of DNA damage. EMBO J 2000;19:463–71.

47. Chen BP, Uematsu N, Kobayashi J, et al. ATM is essential for DNA-pkcs phosphorylations at T2609 cluster upon DNA double strand break. J Biol Chem 2006;282:6582–7.

48. Michel B, Ehrlich SD, Uzest M. DNA double-strand breaks caused by replication arrest. EMBO J 1997;16:430–8.

49. Michel B, Grompone G, Flores MJ, Bidnenko V. Multiple pathways process stalled replication forks. Proc Natl Acad Sci U S A 2004;101:12783–8.